

Supporting Information

Tao et al. 10.1073/pnas.0811648106

Materials and Methods

Antibodies. The commercially available antibodies used are as followed: Mouse monoclonal M2 anti-flag antibody (Sigma), rabbit polyclonal anti-HA antibody (Abcam), mouse monoclonal GAPDH antibody (Abcam), mouse monoclonal actin antibody (Sigma), mouse monoclonal phospho-serine 133-CREB antibody (Cell Signaling), mouse monoclonal CaMK IV antibody (BD transduction), rabbit polyclonal CaMK II antibodies (Santa Cruz, Cell Signaling), mouse monoclonal NeuN antibody (Abcam).

Generation and Initial Analysis of the *Mecp2*^{S80A} and *Mecp2*^{S421A;S424A} Mice. A 5.5-kb SpeI genomic fragment containing part of intron 2, exon 3, intron 3 and exon 4 of the *Mecp2* locus was cloned into pBluescript (\approx 3-kb backbone); a T to G point mutation was introduced in exon 3 by PCR based mutagenesis to change serine 80 to alanine; and a floxed STOP cassette (\approx 2.9 kb) containing the neomycin resistance gene was cloned into intron 2 to make the targeting construct (\approx 11 kb). The targeting construct was linearized and electroporated into mouse ES cells. G418 resistant colonies were picked and expanded for genomic DNA extraction. Southern blot analysis was performed using these genomic DNA samples to examine homologous recombination on both the 5' and 3' arms to identify correctly targeted clones. At least 2 correctly targeted ES cell lines were injected into blastocysts to generate chimeric mice. The chimeric mice were crossed with C57/B6 to obtain germ-line transmission of the LSL-*Mecp2*^{S80A} allele. The LSL-*Mecp2*^{S80A} mice were then crossed with mice carrying a transgenic Cre recombinase allele with germ-line activity to generate *Mecp2*^{S80A} mice. DNA and RNA were extracted from the brains of *Mecp2*^{S80A} mice and their wild type littermates. RNA samples were reverse transcribed into cDNA. PCR reactions were performed using primers designed to specifically amplify the coding region of the *Mecp2* gene that encodes serine 80. Direct sequencing of the PCR or RT-PCR products confirmed the S80A mutation in the *Mecp2*^{S80A} mice. Western blot analysis using S80 specific antibody was used to confirm the absence of phosphorylation at this site in the *Mecp2*^{S80A} mice. Since our mass spectrometry results identified both S421 and S424 phosphorylated in epileptic mouse brains and it was not clear which site was more important at the time we were designing these experiments, we decided to replace both serines with alanines to make a *Mecp2*^{S421A;S424A} mouse. The same strategy and experimental approach used to generate and validate the *Mecp2*^{S80A} mouse were adopted to make the *Mecp2*^{S421A;S424A} mouse.

To test the locomotor function, total dark cycle running wheel activities were recorded in a wheel-running cage connected with a Minicounter (Opto-Varimax-MiniA, Columbus Instruments). For each measurement, a mouse was placed at least 3 h before the starting time into a standard laboratory mouse cage with fresh bedding. Recording started at the time when the lights were normally turned off (19:00 Eastern Standard Time) and stopped at 8:00 the next morning, 1 h after the lights normally came back on.

Plasmids. N-terminal flag-tagged MECP2 human β (e2) form was cloned into pcDNA3.1. C-terminal flag or HA-tagged MeCP2 mouse α (e1) form was cloned into FUIGW lentiviral vector (45) under the control of the ubiquitin promoter. MeCP2 mutants were generated with the Quickchange Site-Directed Mutagenesis Kit (Stratagene).

Cell Culture, Transfection, and Lentiviral Infection. Cortical neurons from E14 or E15 CD1 mice were cultured on polyornithine (Sigma) and fibronectin (GIBCO) coated dishes in Basal Medium Eagle (Sigma) containing 5% FBS, penicillin, streptomycin, glutamine and B27 serum free supplement (Invitrogen). Plasmids or prevalidated SMARTPOOL siRNA (Dharmacon) were electroporated into neurons using Mouse Neuron Nucleofector Kit (Amaxa) with 30% to 50% transfection efficiency. Lentiviruses were produced using the 3rd generation packaging systems as described (Science gateway protocols). E14 or E15 mice cortical neurons were infected with lentiviruses 24 h after dissection and plating. 72–80 h after infection, neurons were treated with drugs and protein/RNA samples were collected.

Seizure Inducement. Eight-week-old male mice (Balb-c) or Long-Evance male rats were given 3 intraperitoneal (i.p.) doses of kainic acid (Sigma-Aldrich, 10 mg/kg body weight) to induce seizure. After 4 h of seizure activity animals were killed. Cortices were quickly removed on dry ice, snap frozen and stored at -80 °C before further experiments.

Immunoblotting. Standard Western blot was performed as described in ref. 46 with modifications. Nuclear extracts were prepared following manufacturer's instructions (Pierce). Whole cell lysates were prepared using SDS lysis buffer (1% SDS, 10 mM EDTA, 50 mM Tris-HCl, pH 8.1) supplemented with protease inhibitor cocktails (Roche), 1 mM PMSF, 1 mM DTT, 50 mM NaF and 1 mM Na₃VO₄. The lysates were immediately pulse sonicated using a microtip (Branson sonifier 450) to break the viscosity caused by chromatin released during the process. Protein concentrations were measured using the BSA Protein Assay Kit (Pierce). The lysates were loaded with SDS sample buffer and size-separated with 8% SDS/PAGE using the 20-cm Protean II xi cell (Bio-Rad) or 10% SDS/PAGE with NuPAGE (Invitrogen). Primary antibodies used were as described in the antibodies section. Secondary goat anti-mouse or anti-rabbit IgG-horseradish antibodies (CalBiochem) were used, and detection was performed using the ECL plus chemiluminescence system (PerkinElmer) on X-Omat Blue films (Kodak). Densitometry analysis was done with Quantity One (Bio-Rad).

Lambda Phosphatase Treatment. Whole cell lysates were harvested in 0.7% Nonidet P-40 lysis buffer (50 mM Tris-HCl, pH 8.0, 0.1 mM EDTA, 250 mM NaCl, 10% glycerol) supplemented with protease inhibitors cocktails (Roche) but not any phosphatase inhibitors. Phosphatase treatment was immediately performed following manufacturer's instructions (NEB).

Drugs. To inhibit basal neuronal activity, 0.5 μ M tetrodotoxin (TTX, Sigma) was applied in the culture medium. 5 μ M KN62 (Calbiochem) was used to inhibit CaM Kinases. 5 μ M nimodipine (Calbiochem) was an L-type Ca²⁺ channel blocker.

Chromatin Immunoprecipitation. Chromatin immunoprecipitation was performed similar as Magna ChIP protocol from Upstate Biotechnologies with modifications. Cortical neurons were cross-linked with 1% formaldehyde for 10 min at room temperature. 0.125M glycine was added at the end of reaction. After 2 washes with cold PBS, cells were lysed with SDS lysis buffer (1% SDS, 10 mM EDTA, 50 mM Tris-HCl, pH 8.1) supplemented with protease inhibitor cocktails (Roche), 1 mM PMSF, 1 mM DTT, 50 mM NaF and 1 mM Na₃VO₄. Cell lysates were

sonicated with a microtip (Branson sonifier 450) until the DNA fragments were \approx 200–1000bp. Sonicated chromatin were diluted till SDS was reduced to <0.1%, and incubated with preimmobilized Protein G Dynabeads (Invitrogen) and antibody complex for overnight at 4 °C. Immunoprecipitates were extensively washed. DNA/protein complexes were eluted from beads and reverse cross-linked at 65 °C. DNA was purified by RNase treatment, proteinase K digestion, phenol/chloroform extraction and precipitated with ethanol and glycogen. The final product was dissolved in 50 μ L of TE. Quantitative PCR was performed with iCycler (Bio-Rad) using iQ SYBR Green supermix (Bio-Rad). PCR efficiencies of primers were examined by standard curve of serial-diluted whole cell extracts input and melting curve functionality. The enrichment was calculated as immunoprecipitation signal versus whole cell lysate input (IP/WCE). The fold changes of MeCP2 mutants ChIP were normalized by MeCP2 wild-type IP/WCE. The ChIP primers used were *Pomc* forward, TACCTCCAAATGCCAGGAAG; *Pomc* reverse, CGCTGGTGGTTAGGAAGAAC; *Gtl2* forward, GAACGTGGCGTAAGATTAGAGG; *Gtl2* reverse, GCT-GTTAAAGTAGCTCGTCAGG; *Vamp3* forward, AAATG-CAGTGGGCTCCTGGTGG; *Vamp3* reverse, CGTCACTGT-TCCAGTCCTCTTGGC; *Rab3d* forward, GCACCGTGTA-AAGCAGCATGGC; *Rab3d* reverse, GCCCACGTGGTGCA-GACAAAAC; *Igsf4b* forward, ACCCAAGCATAA-GAGGGGTGC; *Igsf4b* reverse, CGCGCTTTGTGGTGC-CTTC.

RNA Isolation, Transcription Profiling, and Quantitative RT-PCR. Total RNA was isolated and extracted following manufacturer's instructions (TRIzol, Invitrogen). 4 \times 44k expression array were performed according to manufacturer's instructions (Agilent). 500 ng of total RNA was labeled with Cy3- or Cy5-CTP using the Agilent Low RNA Input Fluorescent Linear Amplification Kit. After labeling and cRNA purification (Qiagen), cRNA was

quantified using the NanoDrop spectrophotometer (Agilent). A total of 825 ng of Cy3- or Cy5-labeled cRNAs were combined and hybridized to the Agilent 4 \times 44K whole mouse genome microarray (G412F) for 17 h at 65 °C (10 rpm). Data were collected using Agilent microarray scanner and extracted with Feature Extraction 9.1 software (Agilent). Experiments were performed in triplicate using biologically independent cultures, with a dye-swap design used. For identification of differentially expressed genes, we used NIA array analysis tool (<http://lgsun.grc.nia.nih.gov/ANOVA>). The following parameters were used for analyzing statistically significant differential expression: threshold z value to remove outliers: 10,000; error model: max (average, Bayesian); error variance averaging window: 200; proportion of highest error variances to be removed: 0.01; Bayesian degrees of freedom: 5; false discovery rate (FDR) threshold: 0.05 or 0.1. The microarray data have been deposited in the NCBI Gene Expression Omnibus (GEO) and are accessible through GEO series accession number GSE14715. One to 2 micrograms of total RNA was used for cDNA synthesis using SuperScript III (Invitrogen) following manufacturer's protocol. Quantitative RT-PCR was performed with iCycler (Bio-Rad) using iQ SYBR Green supermix (Bio-Rad). PCR efficiencies of primers were examined by standard curve of serial-diluted cDNA and melting curve functionality. The mRNA levels were normalized for each well to the Gapdh mRNA levels. Primers used were: *Pomc* forward, CATTAGGCTTGGAG-CAGGTC; *Pomc* reverse, CTTCTCGGAGGTATGAAGC; *Gtl2* forward, CCCTCAGATCAGGCTTCAAC; *Gtl2* reverse, CCACTCCTACTGGCTGCTC; *Vamp3* forward, TTGAAA-CAAGTGCTGCCAAG; *Vamp3* reverse, GAGACAC-ACCACACGATGATG; *Rab3d* forward, GCTATGCCGATGATCCTTC; *Rab3d* reverse, AGTAGGCCGTGGTATTGTC; *Igsf4b* forward, GCAGTGGTCTAACCTGCTC; *Igsf4b* reverse, TTCGCACAGGCATAGTGAAG; *Gapdh* forward, CTGAG-TATGTCGTGGAGTCTACTGG; *Gapdh* reverse, GTCATATT-TCTCGTGGTTCACACC.

A**B**

Cell type	Phosphorylation sites identified by MS
HeLa cell	S80
PC12 cell	S80, T148/S149, S164, S216, S229, S399

Fig. S1. (A) Protein sequence alignment of e1 forms of human, mouse and rat MeCP2. The sites shaded in red were identified in normal mouse brain samples while the sites shaded in green were identified in seized mouse brain samples. The corresponding sites in MeCP2 e2 form were marked with numeration. (B) Phosphorylation sites of endogenous MeCP2 identified from HeLa cells and PC12 cells.

Mouse normal brain

MVAGMLGLREEK**SEDQDLQGLRDKPLKF**KKKAKKDKKEDKEGKHEPLQPSAH**HSAEPAEAGKAETSESSGS**
APAVPEASASPQQRRSIIRDRGPMYDDPTLPEGWTRKLQRKSGRSAGKYDVYLINPQGKAFRSKVELIA
YFEKVGDTSLPNDFDFTVTGRGSPSRREQKPPKKPKSPKAPGTGRGRGRPKGSGTGRPKAAASEGVQVK
RVLEKSPGKLVVKMFPQASPGGGEGGGATTSAQVMVIKRPGRKRAEADPQAIPKRKRGKPGSVAAAA
AEAKKAVKESSIRSVHETVLPIKKRKTRTVSIEVKEVVKPLLVSTLGEKSGKGLKTCSPGRKSKESS
PKGRSSSASSPPKKEHHHHHHHSEST**KAPMPLLPSPPP**PEPESSEDPISPPEPQDLSSSICKEEKMPRGG
SLESDGCPKEPAKTQPMVATTTVAEKYKHRGEGERKDIVSSMMPRNREEPVDSRTPVTERVS

Mouse seized brain lower band

MVAGMLGLREEK**SEDQDLQGLRDKPLKF**KKKAKKDKKEDKEGKHEPLQPSAH**HSAEPAEAGKAETSESSGS**
APAVPEASASPQQRRSIIRDRGPMYDDPTLPEGWTRKLQRKSGRSAGKYDVYLINPQGKAFRSKVELIA
YFEKVGDTSLPNDFDFTVTGRGSPSRREQKPPKKPKSPKAPGTGRGRGRPKGSGTGRPKAAASEGVQVK
RVLEKSPGKLVVKMFPQASPGGGEGGGATTSAQVMVIKRPGRKRAEADPQAIPKRKRGKPGSVAAAA
AEAKKAVKESSIRSVHETVLPIKKRKTRTVSIEVKEVVKPLLVSTLGEKSGKGLKTCSPGRKSKESS
PKGRSSSASSPPKKEHHHHHHHSEST**KAPMPLLPSPPP**PEPESSEDPISPPEPQDLSSSICKEEKMPRGG
SLESDGCPKEPAKTQPMVATTTVAEKYKHRGEGERKDIVSSMMPRNREEPVDSRTPVTERVS

Mouse seized brain upper band

MVAGMLGLREEK**SEDQDLQGLRDKPLKF**KKKAKKDKKEDKEGKHEPLQPSAH**HSAEPAEAGKAETSESSGS**
APAVPEASASPQQRRSIIRDRGPMYDDPTLPEGWTRKLQRKSGRSAGKYDVYLINPQGKAFRSKVELIA
YFEKVGDTSLPNDFDFTVTGRGSPSRREQKPPKKPKSPKAPGTGRGRGRPKGSGTGRPKAAASEGVQVK
RVLEKSPGKLVVKMFPQASPGGGEGGGATTSAQVMVIKRPGRKRAEADPQAIPKRKRGKPGSVAAAA
AEAKKAVKESSIRSVHETVLPIKKRKTRTVSIEVKEVVKPLLVSTLGEKSGKGLKTCSPGRKSKESS
PKGRSSSASSPPKKEHHHHHHHSEST**KAPMPLLPSPPP**PEPESSEDPISPPEPQDLSSSICKEEKMPRGG
SLESDGCPKEPAKTQPMVATTTVAEKYKHRGEGERKDIVSSMMPRNREEPVDSRTPVTERVS

Rat normal brain

MVAGMLGLREEK**SEDQDLQGLKEKPLKF**KKVKKDKKEDKEGKHEPLQPSAH**HSAEPAEAGKAETSESSGS**
APAVPEASASPQQRRSIIRDRGPMYDDPTLPEGWTRKLQRKSGRSAGKYDVYLINPQGKAFRSKVELIA
YFEKVGDTSLPNDFDFTVTGRGSPSRREQKPPKKPKSPKAPGTGRGRGRPKGSGTGRPKAAASEGVQVK
RVLEKSPGKLLVKMFPQASPGGGEGGGATTSAQVMVIKRPGRKRAEADPQAIPKRKRGKPGSVAAAA
AEAKKAVKESSIRSVQETVLPIKKRKTRTVSIEVKEVVKPLLVSTLGEKSGKGLKTCSPGRKSKESS
PKGRSSSASSPPKKEHHHHHHHAESP**KAPMPLLPPP**PEPQSSEDPISPPEPQDLSSSICKEEKMPRAG
SLESDGCPKEPAKTQPMVAAAATTTTTTTVAEKYKHRGEGERKDIVSSMMPRNREEPVDSRTPVTER
 VS

Rat seized brain lower band

MVAGMLGLREEK**SEDQDLQGLKEKPLKF**KKVKKDKKEDKEGKHEPLQPSAH**HSAEPAEAGKAETSESSGS**
APAVPEASASPQQRRSIIRDRGPMYDDPTLPEGWTRKLQRKSGRSAGKYDVYLINPQGKAFRSKVELIA
YFEKVGDTSLPNDFDFTVTGRGSPSRREQKPPKKPKSPKAPGTGRGRGRPKGSGTGRPKAAASEGVQVK
RVLEKSPGKLLVKMFPQASPGGGEGGGATTSAQVMVIKRPGRKRAEADPQAIPKRKRGKPGSVAAAA
AEAKKAVKESSIRSVQETVLPIKKRKTRTVSIEVKEVVKPLLVSTLGEKSGKGLKTCSPGRKSKESS
PKGRSSSASSPPKKEHHHHHHHAESP**KAPMPLLPPP**PEPQSSEDPISPPEPQDLSSSICKEEKMPRAG
SLESDGCPKEPAKTQPMVAAAATTTTTTTVAEKYKHRGEGERKDIVSSMMPRNREEPVDSRTPVTER
 VS

Rat seized brain upper band

MVAGMLGFREEK**SEDQDLQGLKEKPLKF**KKVKKDKKEDKEGKHEPLQPSAH**HSAEPAEAGKAETSESSGS**
APAVPEASASPQQRRSIIRDRGPMYDDPTLPEGWTRKLQRKSGRSAGKYDVYLINPQGKAFRSKVELIA
YFEKVGDTSLPNDFDFTVTGRGSPSRREQKPPKKPKSPKAPGTGRGRGRPKGSGTGRPKAAASEGVQVK
RVLEKSPGKLLVKMFPQASPGGGEGGGATTSAQVMVIKRPGRKRAEADPQAIPKRKRGKPGSVAAAA
AEAKKAVKESSIRSVQETVLPIKKRKTRTVSIEVKEVVKPLLVSTLGEKSGKGLKTCSPGRKSKESS
PKGRSSSASSPPKKEHHHHHHHAESP**KAPMPLLPPP**PEPQSSEDPISPPEPQDLSSSICKEEKMPRAG
SLESDGCPKEPAKTQPMVAAAATTTTTTTVAEKYKHRGEGERKDIVSSMMPRNREEPVDSRTPVTER
 VS

Fig. S2. Mass spectrometry coverage chart with identified peptides shaded in red.

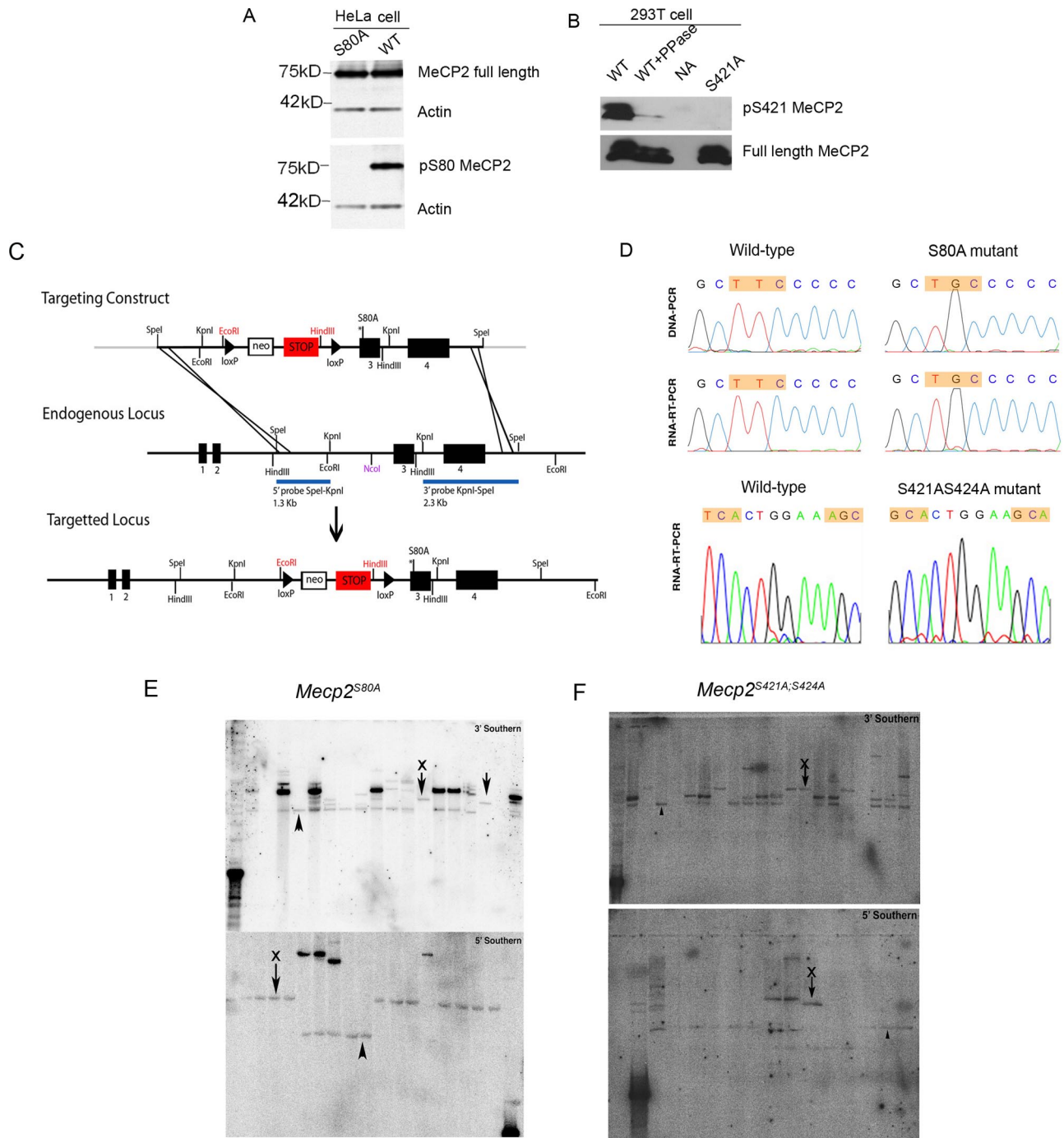


Fig. S3. Characterization of MeCP2 serine 80, serine 421 phospho-specific antibodies and *Mecp2*^{S80A} and *Mecp2*^{S421AS424A} knock-in mice. (A) Wild-type and S80A MeCP2 were transfected into HeLa cells that expressed a very low level of endogenous MeCP2. Western blot with phospho-S80 antibody recognized the band of wild type protein but not the S80A mutant. The same membrane was stripped and blotted with full length MeCP2 antibody afterward. (B) Wild-type and S421A MeCP2 were transfected into 293T cells that had a low level of endogenous MeCP2. Phospho-S421 antibody detected doublet bands of wild-type MeCP2 that were sensitive to phosphatase treatment, but failed to detect any band in S421A MeCP2. It is possible that 293T cells may have different posttranslational modifications of MeCP2 as both phospho-S421 and full length MeCP2 antibodies detected doublet bands at basal level. (C) Illustration of the targeting strategy for making an LSL-Mecp2^{S80A} allele. Grey sections on the targeting construct indicate sequence of plasmid origin. Restriction sites in red are on the stop cassette. (D) Sequencing results from genomic DNA and RNA level confirm the successful engineering of the serine 80 to alanine mutation in the *Mecp2*^{S80A} mouse brain and the serine 421 and serine 424 to alanine mutation in the *Mecp2*^{S421AS424A} mouse brain. (E and F) Southern blot analysis to identify ES cell clones that are correctly targeted at the endogenous *Mecp2* locus. On top is the Southern blot analysis of the 3' arm of the endogenous *Mecp2* locus; at the bottom is the Southern blot analysis of the 5' arm of the locus. Arrowheads indicate the wild type *Mecp2* alleles. Arrows indicate the LSL-*Mecp2*^{S80A} alleles (E) or the LSL-*Mecp2*^{S421AS424A} alleles (F). X indicates the same ES cell clone that is correct on both the 3' and 5' arms. In either the wild-type clones or the correctly targeted clone, only 1 band (allele) is seen, because the *Mecp2* gene is located on the X chromosome and the parental ES cell line is male and has only 1 X chromosome.

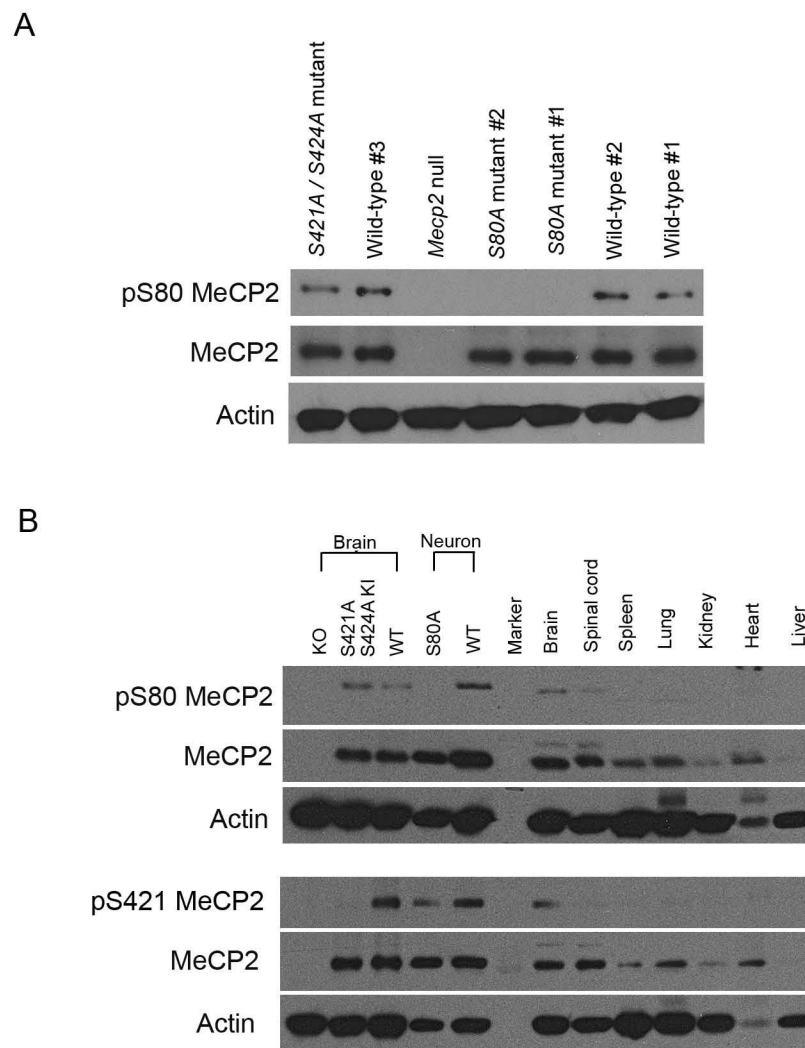


Fig. S4. (A) MeCP2 protein expression levels from brain extracts of *Mecp2*^{S80A}, *Mecp2*^{S421AS424A} and their wild-type littermates are similar. *Mecp2*^{S80A} (#1,#2) and wild type littermate (#1, #2) were 5 months old. *Mecp2*^{S421AS424A} and its wild type litter mate (#3) were 3 months old. (B) Expression levels of MeCP2 and its phosphorylated forms in various tissues isolated from 3-month-old wild type mice.

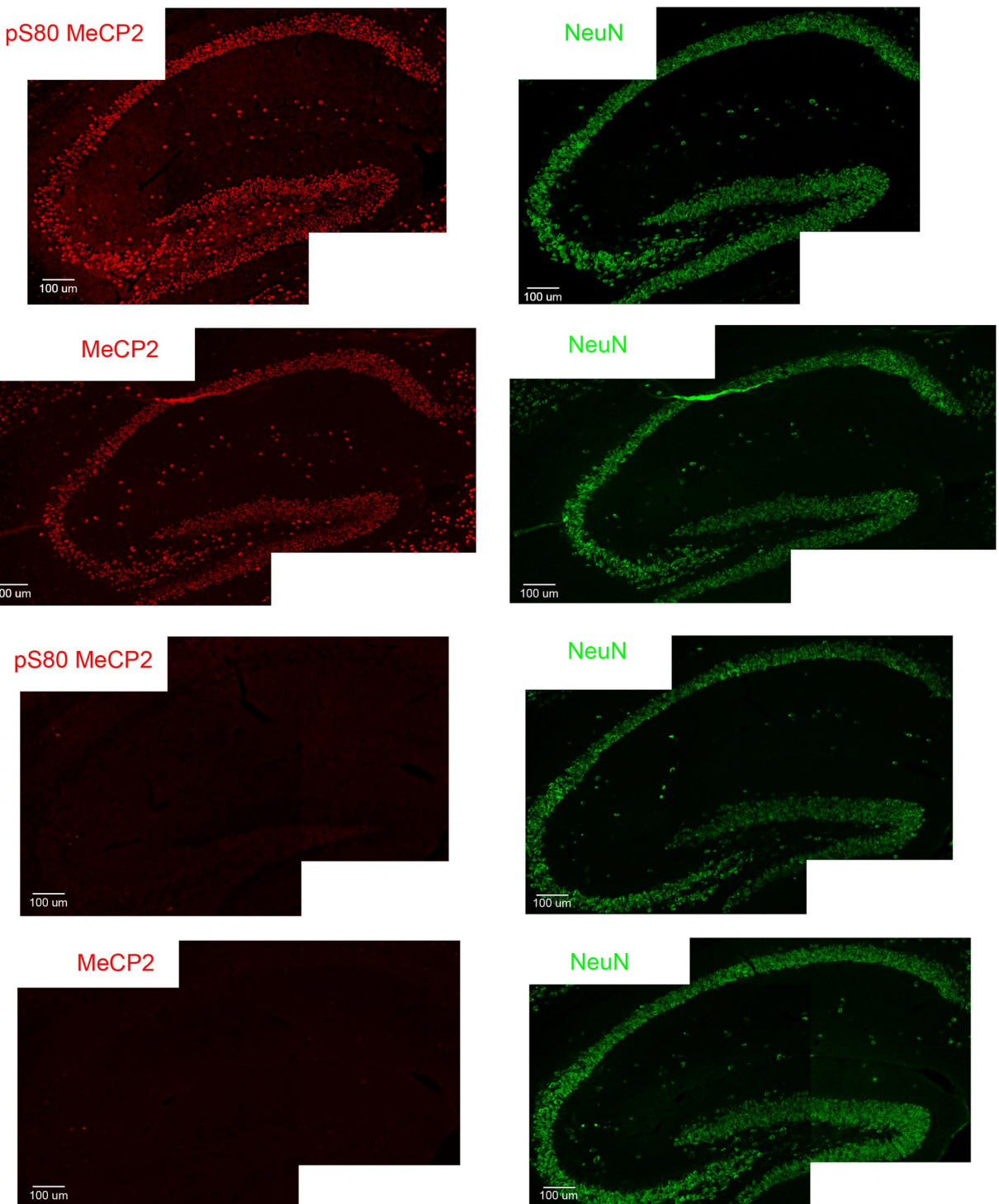


Fig. S5. Immunostainings of postnatal 3 weeks old mouse hippocampal region with neuronal marker NeuN, phospho-S80 MeCP2 and Upstate C-terminal MeCP2 antibody respectively. Comparable *Mecp2* $-/y$ sections served as negative controls.

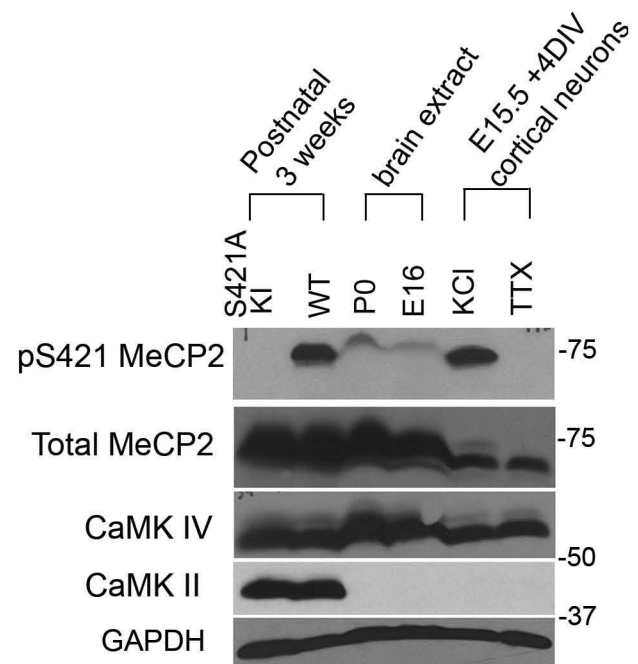


Fig. S6. Protein levels of MeCP2 phospho-S421, CaMK II and CaMK IV at different developmental stages. Western blot was done with lysates of E15.5 + 4DIV cultured mouse cortical neurons with TTX or KCl treatment, E16 and P0 brain extracts, postnatal 3-weeks-old wild type and S421A mutant mice brain extracts, respectively.

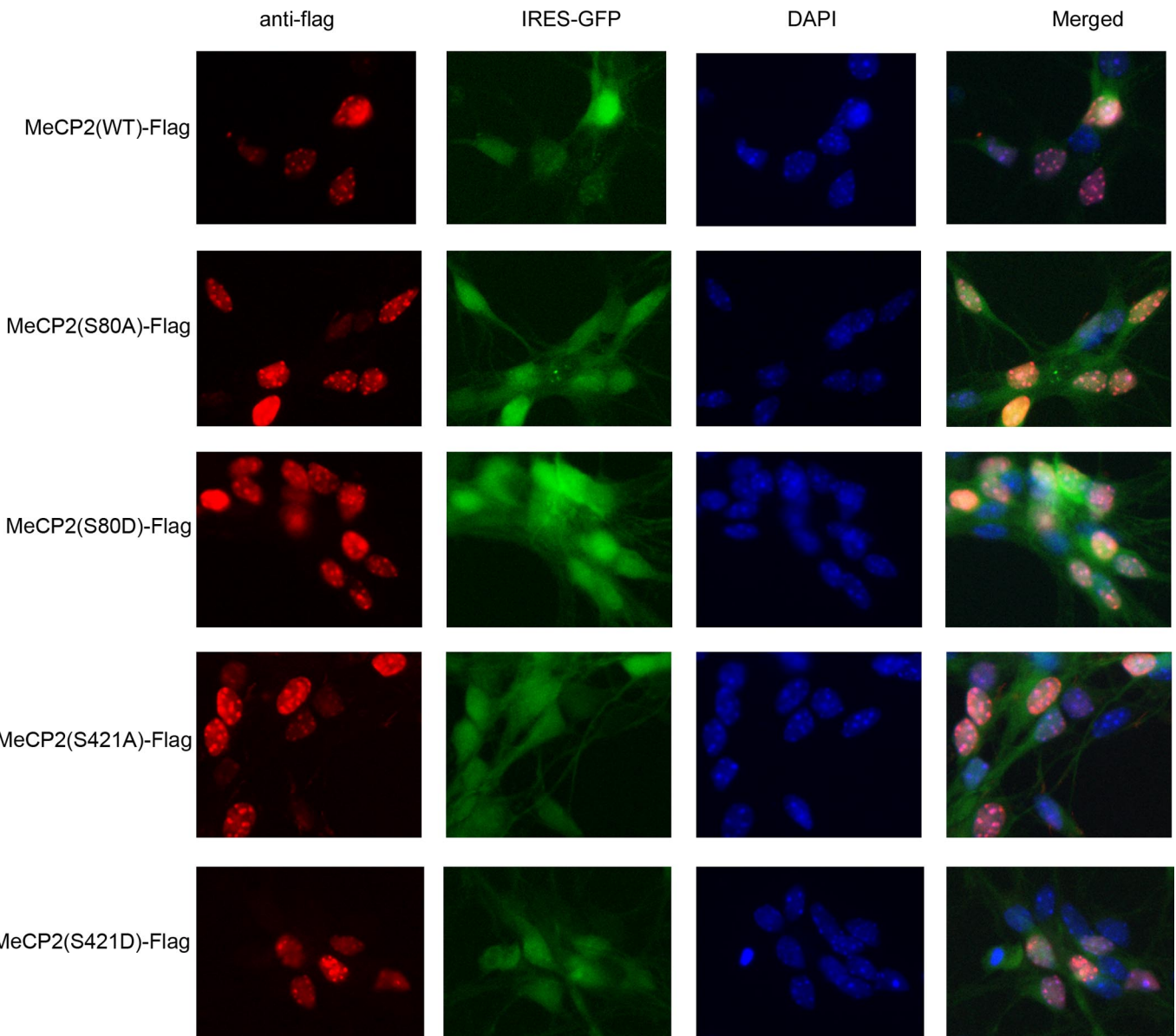
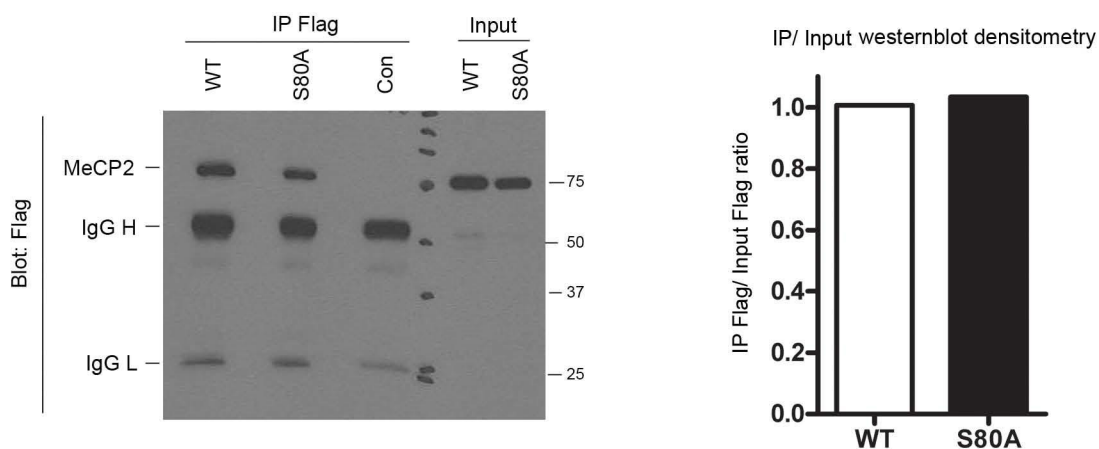


Fig. S7. Immunostainings of flag-tagged wild-type or S80/S421 phosphorylation site mutant MeCP2 in resting neurons did not show global distribution changes. Lentivirus infected neurons also express GFP.

A



B

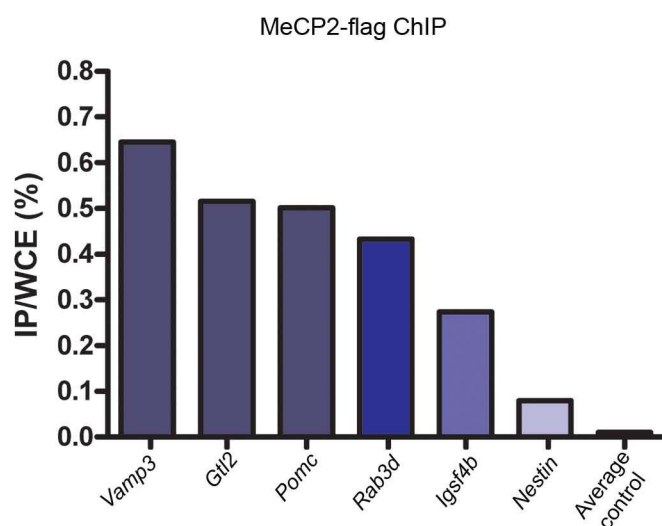


Fig. S8. Chromatin immunoprecipitation with the flag antibody is specific. (A) Western blot following immunoprecipitation under ChIP condition with mouse cortical neurons showed that both wild-type and S80A MeCP2 could be immunoprecipitated with similar efficiency. (B) MeCP2 showed different binding affinities at different promoters. Dark blue shaded promoters (*Vamp3*, *Gtl2* and *Pomp*) are relatively high affinity binding targets. Medium to light blue shaded promoters (*Rab3d* and *Igsf4b*) are relatively medium to low affinity binding targets. Very light blue shaded *Nestin* promoter served as a negative control with very low binding affinity. Flag immunoprecipitation from no flag-tagged MeCP2 neurons served as the average control.

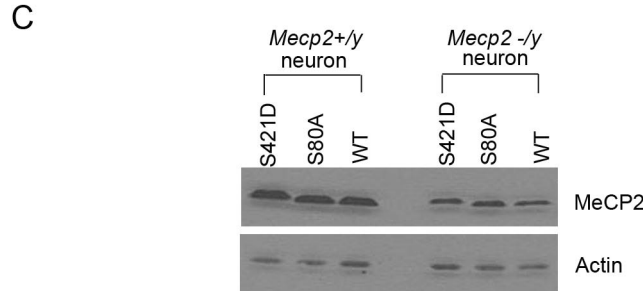
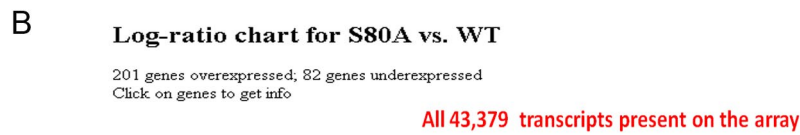
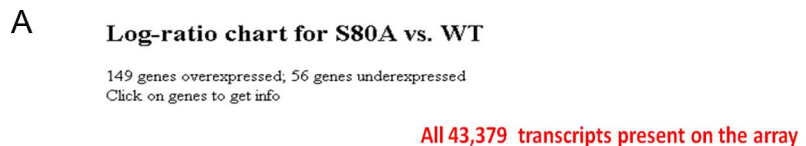


Fig. S9. Transcriptional profiling of *Mecp2* null mouse cortical neurons rescued with wild-type and phosphorylation site mutant MeCP2. Log-ratio charts showed the distribution of up-regulated and down-regulated genes of neurons expressing MeCP2 S80A versus those expressing wild-type MeCP2 with FDR at 0.05 (A) and FDR at 0.1 (B) respectively. (C) *Mecp2* null cortical neurons rescued with wild-type and mutant MeCP2 showed similar levels of exogenous MeCP2 expression, which are approximately the same level compared with the wild-type neurons.

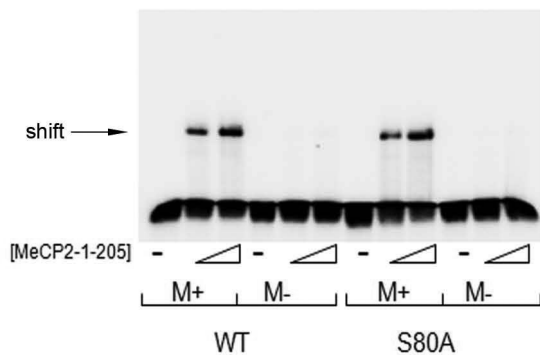


Fig. S10. EMSA analysis suggested that S80A mutation did not affect MeCP2 MBD binding to naked methylated DNA oligos. The methylated probe used was the S1 probe used as described in previous publication [Klose RJ, et al. (2005) DNA binding selectivity of MeCP2 due to a requirement for A/T sequences adjacent to methyl-CpG. *Mol Cell* 19:667–678.] GCAGCACGGTGGGGGGCC**G**AGTTAAGGACTCGTTGTC. Bold CCGG were methylated. M+ and M- indicated the presence or absence of methyl-CpG in the EMSA fragment. The concentration of MeCP2 was indicated below and (-) indicated free probe. Recombinant human MECP2 amino acid 1–205 wild-type or S80A purified from bacteria were used.

Table S1. Comparison of *Mecp2* mutant mice

	<i>Mecp2</i> <i>-/y</i> by Jaenisch group (1)	<i>Mecp2</i> <i>-/y</i> by Bird group (2)	<i>Mecp2</i> 308/ <i>y</i> (3)	<i>Mecp2</i> 580/ <i>A/y</i>	<i>Mecp2</i> <i>S421AS424A/y</i>
Mouse strain	C57BL/6J, 129/Sv and Balb/c	C57BL/6J	C57BL/6J, 129/Sv	C57BL/6J, 129/Sv	C57BL/6J, 129/Sv
Life span	Death between 6 to 12 weeks of age	Death around postnatal 54 days	Most survived to 1 year of age	Normal life span	Normal life span
Body and brain weights	Reduced brain weight and smaller neuronal cell sizes. Gain of body weight at early symptomatic stage and loss of weight at late stage.	Varying body weight	Normal brain and body weight	Normal brain weight and slightly heavier body weight	Slightly heavier brain weight and normal body weight
Symptoms onset time	5 weeks of age	3–8 weeks of age	Subtle tremor at 6 weeks of age; apparent at 4 months of age	2–3 months of age	2–3 months of age
Phenotypes	Body trembling, hypoactive, hard respiration, ataxia gait.	Stiff and uncoordinated gait, reduced spontaneous movement, hindlimb clasping, irregular breathing.	Tremors, motor impairments, hypoactivity, increased anxiety-related behavior, seizures, kyphosis and stereotypic forelimb motions.	Reduced locomotor activity*	Increased locomotor activity*

*Further full scale behavior characteristics remain to be determined.

- Chen RZ, Akbarian S, Tudor M, Jaenisch R (2001) Deficiency of methyl-CpG binding protein 2 in CNS neurons results in a Rett-like phenotype in mice. *Nat Genet* 27:327–331.
- Guy J, Hendrich B, Holmes M, Martin JE, Bird A (2001) A mouse *Mecp2*-null mutation causes neurological symptoms that mimic Rett Syndrome. *Nat Genet* 27:322–326.
- Shahbazian M, et al. (2002) Mice with truncated MeCP2 recapitulate many Rett Syndrome features and display hyperacetylation of histone H3. *Neuron* 35:243–254.

Table S2. Genes that are up-regulated in S80A samples compared with wild-type samples which may contain multiple probes targeting the same gene

Symbol	Annotation	Mean (S80A)	Mean (WT)	Log Ratio	Fold Change	FDR
Genes that are up-regulated in S80A samples compared with wild-type samples (FDR < 0.05)						
Arl15	NM_172595	4.0235	3.4914	0.5321	3.404	0
Vapb	NM_019806	4.0942	3.59151	0.50269	3.181	0
Ube2s	AK003078	4.3967	3.94831	0.44839	2.807	0
Ube2s	NM_133777	4.3203	3.89831	0.42199	2.642	0
Ddit4	NM_029083	4.5083	4.1408	0.3675	2.33	0
Igfsf4b	NM_053199	3.3031	2.8497	0.4534	2.84	0
Chmp4b	NM_029362	3.3969	3.00531	0.39159	2.463	0
Cbx8	AK051905	3.6363	3.27861	0.35769	2.278	0
Cd93	NM_010740	2.0501	1.3441	0.706	5.081	0
Rgag4	NM_183318	3.2206	2.8646	0.356	2.269	0
Arl15	NM_172595	2.3156	1.79011	0.52549	3.353	0
2400003N08Rik	NM_178622	3.4424	3.1342	0.3082	2.033	0
BC017612	NM_133214	2.6209	2.2234	0.3975	2.497	0
Rab5c	NM_024456	3.8966	3.64781	0.24879	1.773	0
Car3	NM_007606	1.7327	1.0611	0.6716	4.694	0
Tcf25	NM_025804	4.661	4.46511	0.19589	1.569	0.0046
Rpo1-2	NM_009086	2.7401	2.4276	0.3125	2.053	0
Odf2	BC057001	3.2338	2.9739	0.2599	1.819	0.0006
Sympk	BC049852	3.4027	3.15771	0.24499	1.757	0
Odf2	BC057001	2.9472	2.6675	0.2797	1.904	0.003
Tcf25	NM_025804	3.9199	3.71601	0.20389	1.599	0.0164
Mpst	NM_138670	3.2991	3.0624	0.2367	1.724	0
Setd5	NM_028385	4.1714	3.9884	0.183	1.524	0
Gm1752	XM_001003685	2.0884	1.6978	0.3906	2.458	0
Tspyl1	NM_009433	3.9586	3.7672	0.1914	1.553	0.0002
Nans	NM_053179	3.4225	3.20001	0.22249	1.669	0
Med18	NM_026039	2.9089	2.6437	0.2652	1.841	0.0001
2810482G21Rik	AK122545	2.7054	2.419	0.2864	1.933	0
Arl6ip5	NM_022992	3.7976	3.5997	0.1979	1.577	0.0004
Vamp3	NM_009498	2.5043	2.1942	0.3101	2.042	0.0005
Rab3d	NM_031874	2.7433	2.46791	0.27539	1.885	0
Rian	AK017440	3.5411	3.3383	0.2028	1.595	0.0145
AK143126	AK143126	2.2967	1.9704	0.3263	2.119	0
Tatdn2	NM_001033463	2.9354	2.6879	0.2475	1.768	0
AK046873	AK046873	2.3955	2.0872	0.3083	2.033	0
NAP057026-1	NAP057026-1	2.404	2.09791	0.30609	2.023	0
Rnf20	NM_182999	3.1599	2.94071	0.21919	1.656	0.0014
Zswim6	BC021311	2.9449	2.70991	0.23499	1.717	0
Fgr	NM_010208	2.0997	1.75521	0.34449	2.21	0.0007
Igfsf4c	NM_153112	3.6004	3.4112	0.1892	1.545	0
5830457O10Rik	NM_145412	2.5089	2.2319	0.277	1.892	0
Supt7l	NM_028150	2.0734	1.73091	0.34249	2.2	0
B4galnt7	NM_146045	2.6143	2.3541	0.2602	1.82	0
Polh	NM_030715	1.5822	1.1015	0.4807	3.024	0
Vapb	NM_019806	2.4449	2.1668	0.2781	1.897	0
Cntn2	NM_177129	3.8167	3.6481	0.1686	1.474	0.0002
2610200G18Rik	NM_025998	2.3788	2.10021	0.27859	1.899	0
LOC665155	XM_976391	1.7638	1.3713	0.3925	2.468	0
Kif15	NM_010620	2.7726	2.5416	0.231	1.702	0.0004
Lix1	BC063057	2.5354	2.2814	0.254	1.794	0.0003
Cpxl2	NM_009946	3.1035	2.9004	0.2031	1.596	0.0052
Snap29	NM_023348	3.6546	3.48381	0.17079	1.481	0.0011
AK050977	AK050977	2.6763	2.43881	0.23749	1.727	0
Fgd4	AK042588	2.0955	1.78331	0.31219	2.052	0.0001
Bloc1s3	NM_177692	2.5802	2.3345	0.2457	1.76	0
Med18	NM_026039	2.713	2.48221	0.23079	1.701	0.0001
Ly6h	NM_011837	3.5055	3.3301	0.1754	1.497	0.0184
Aco1	NM_007386	2.4103	2.14741	0.26289	1.831	0.0001
Lsm14b	NM_177727	2.6059	2.36521	0.24069	1.74	0.0035
Pafah1b1	NM_013625	4.2438	4.1015	0.1423	1.387	0.0031
Ufd1l	NM_011672	2.583	2.3464	0.2366	1.724	0.0305

Symbol	Annotation	Mean (S80A)	Mean (WT)	Log Ratio	Fold Change	FDR
Stk32c	NM_021302	1.8192	1.46541	0.35379	2.258	0
Pigt	NM_133779	4.1392	3.99691	0.14229	1.387	0.0209
Raf1	AK036317	2.5964	2.36601	0.23039	1.699	0
TC1522927	TC1522927	1.9304	1.60751	0.32289	2.103	0
Psmd9	NM_026000	2.8406	2.63381	0.20679	1.609	0.0256
TC1477251	TC1477251	1.434	0.97431	0.45969	2.881	0.0003
E430012M05Rik	AK051077	1.5833	1.19081	0.39249	2.468	0.0124
G430041M01Rik	NM_198102	2.9468	2.7561	0.1907	1.551	0
Rad1	NM_011232	2.7436	2.5401	0.2035	1.597	0.0003
AK043110	AK043110	2.6822	2.4751	0.2071	1.611	0.0221
AK084126	AK084126	1.3788	0.9132	0.4656	2.921	0.0018
ENSMUST00000088292	ENSMUST00000088292	2.8102	2.6148	0.1954	1.568	0.0101
Rgs16	NM_011267	2.9383	2.75491	0.18339	1.525	0
Cdk6	NM_009873	1.64	1.28761	0.35239	2.251	0.0089
ENSMUST00000066134	ENSMUST00000066134	3.6712	3.52821	0.14299	1.389	0.003
Peo1	NM_153796	1.6882	1.35021	0.33799	2.177	0
Rab11b	NM_008997	2.5199	2.30881	0.21109	1.625	0.0387
U2af2	NM_133671	2.1962	1.9526	0.2436	1.752	0.0017
Hnrpa0	AK019388	3.069	2.90181	0.16719	1.469	0.001
Paxip1	NM_018878	1.4839	1.09991	0.38399	2.42	0.0199
Sh3bp2	NM_011893	2.5914	2.39321	0.19819	1.578	0.0236
Map3k10	XM_887283	3.5426	3.4005	0.1421	1.387	0.0073
Gas2l3	AK018456	2.6355	2.44181	0.19369	1.562	0.0374
2410081M15Rik	NM_028603	3.025	2.85821	0.16679	1.468	0.0006
Gabbr1	BC054735	2.8551	2.6808	0.1743	1.493	0.0272
Slc8a2	NM_148946	2.2588	2.03411	0.22469	1.677	0.0006
Ing3	NM_023626	2.5752	2.3815	0.1937	1.562	0.0009
6430526N21Rik	NM_001033383	2.4639	2.2607	0.2032	1.596	0.0015
Srebf2	NM_033218	3.0197	2.85781	0.16189	1.451	0.0002
Ube2b	AK135056	2.3598	2.15171	0.20809	1.614	0
Ccdc49	NM_026186	2.6446	2.4617	0.1829	1.523	0.0058
Bcl9	AK147659	2.4209	2.2216	0.1993	1.582	0.0004
AK169992	AK169992	1.9518	1.69871	0.25309	1.79	0.0005
Rbm9	NM_175387	3.4147	3.27721	0.13749	1.372	0.0005
Metrn	NM_133719	3.0922	2.9404	0.1518	1.418	0.0077
Chst7	NM_021715	2.5493	2.3629	0.1864	1.536	0.0053
Polr3gl	NM_027241	3.597	3.46741	0.12959	1.347	0.0483
BB113933	BB113933	3.0154	2.8596	0.1558	1.431	0.0004
Hnrpa0	AK019388	2.4619	2.26901	0.19289	1.559	0.0085
Olig1	NM_016968	3.0919	2.9429	0.149	1.409	0.0103
Cyp26a1	NM_007811	1.3164	0.9226	0.3938	2.476	0.0314
Osbpl8	NM_175489	2.6326	2.46051	0.17209	1.486	0.0237
AK030273	AK030273	2.6977	2.5313	0.1664	1.466	0.0011
BC024868	NM_199149	3.0649	2.9198	0.1451	1.396	0.04
Cxadr	NM_001025192	3.2273	3.0925	0.1348	1.363	0.0016
Fbln2	NM_007992	2.7746	2.61891	0.15569	1.431	0.0062
Acads	NM_007383	2.1065	1.897	0.2095	1.619	0.0029
ENSMUST00000098637	ENSMUST00000098637	2.3	2.11051	0.18949	1.546	0.005
Fbxo30	NM_027968	3.0447	2.905	0.1397	1.379	0.008
Slc27a1	NM_011977	2.946	2.8021	0.1439	1.392	0.0015
Tigd3	NM_198634	1.7684	1.51781	0.25059	1.78	0.01
0610011I04Rik	NM_025326	2.0326	1.8194	0.2132	1.633	0.006
Igf2bp1	NM_009951	2.6447	2.48871	0.15599	1.432	0.001
Zfp146	NM_011980	2.1809	1.98901	0.19189	1.555	0.0016
C79127	NM_177691	1.7607	1.51971	0.24099	1.741	0.0157
2810474O19Rik	NM_026054	3.6486	3.53901	0.10959	1.287	0.0083
AK129128	AK079259	1.3877	1.0695	0.3182	2.08	0.0452
Unc5b	NM_029770	2.1387	1.9494	0.1893	1.546	0.0006
Cdca7l	NM_146040	1.6623	1.4124	0.2499	1.777	0.0192
A_52_P893105	A_52_P893105	1.9018	1.68781	0.21399	1.636	0.0011
TC1521263	TC1521263	2.532	2.37571	0.15629	1.433	0.001
1500009C09Rik	XM_901682	2.6204	2.4701	0.1503	1.413	0.0086
Trip10	NM_134125	1.3637	1.04631	0.31739	2.076	0.022
Zic1	NM_009573	3.0761	2.94931	0.12679	1.339	0.0374

Symbol	Annotation	Mean (S80A)	Mean (WT)	Log Ratio	Fold Change	FDR
BU562039	BU562039	2.7349	2.59161	0.14329	1.39	0.0243
Cyp20a1	NM_030013	2.3133	2.1424	0.1709	1.482	0.0086
Gipr	AK146552	1.3041	0.9693	0.3348	2.161	0.0413
Igf1r	NM_010513	2.5654	2.41351	0.15189	1.418	0.0198
Wasl	NM_028459	2.504	2.35151	0.15249	1.42	0.0006
Soat1	NM_009230	1.9139	1.71101	0.20289	1.595	0.0405
AI461788	AK028016	1.2278	0.8805	0.3473	2.224	0.0418
Mical2	NM_177282	1.743	1.5209	0.2221	1.667	0.0483
Ceecam1	NM_207298	1.9488	1.7543	0.1945	1.564	0.018
Tbc1d9	NM_027758	1.777	1.56151	0.21549	1.642	0.0147
Kpna4	NM_008467	1.82	1.6176	0.2024	1.593	0.0272
Snf1lk	NM_010831	2.6865	2.5556	0.1309	1.351	0.0362
0710001B24Rik	NM_175118	2.6386	2.50531	0.13329	1.359	0.0322
BC021831	BC021831	1.8534	1.65831	0.19509	1.567	0.0304
Cnr1	NM_007726	2.3633	2.2138	0.1495	1.41	0.0039
AK044799	AK044799	1.892	1.70171	0.19029	1.549	0.0077
TC1440691	TC1440691	2.4368	2.29251	0.14429	1.394	0.0051
Calcoco1	NM_026192	1.9762	1.79781	0.17839	1.507	0.024
Rdh13	AK089458	2.0336	1.86151	0.17209	1.486	0.0063
Zbtb24	AF263010	2.3131	2.1651	0.148	1.406	0.0088
Arvcf	NM_033474	2.904	2.78831	0.11569	1.305	0.0036
AK037868	AK037868	1.7816	1.5865	0.1951	1.567	0.0431
Mapk8	NM_016700	2.2339	2.0824	0.1515	1.417	0.0488
Peg3	NM_008817	2.1974	2.046	0.1514	1.417	0.0292
Snx27	AK147452	1.8533	1.67501	0.17829	1.507	0.0359
D030051J21Rik	AK083595	1.1949	0.8988	0.2961	1.977	0.0346
Chd1	NM_007690	2.1572	2.01	0.1472	1.403	0.0477
Gsk3b	NM_019827	2.3586	2.22501	0.13359	1.36	0.0127
Lrrc57	NM_025657	2.3637	2.2332	0.1305	1.35	0.0094
Stch	NM_030201	2.8925	2.7943	0.0982	1.253	0.024
6430704M03Rik	AK078331	2.1056	1.97551	0.13009	1.349	0.0483
Genes that are up-regulated in S80A samples compared with wild-type samples (FDR < 0.1)						
Arl15	NM_172595	4.0235	3.4914	0.5321	3.404	0
Vapb	NM_019806	4.0942	3.59151	0.50269	3.181	0
Ube2s	AK003078	4.3967	3.94831	0.44839	2.807	0
Ube2s	NM_133777	4.3203	3.89831	0.42199	2.642	0
Ddit4	NM_029083	4.5083	4.1408	0.3675	2.33	0
Igfs4b	NM_053199	3.3031	2.8497	0.4534	2.84	0
Chmp4b	NM_029362	3.3969	3.00531	0.39159	2.463	0
Cbx8	AK051905	3.6363	3.27861	0.35769	2.278	0
Cd93	NM_010740	2.0501	1.3441	0.706	5.081	0
Rgag4	NM_183318	3.2206	2.8646	0.356	2.269	0
Arl15	NM_172595	2.3156	1.79011	0.52549	3.353	0
2400003N08Rik	NM_178622	3.4424	3.1342	0.3082	2.033	0
BC017612	NM_133214	2.6209	2.2234	0.3975	2.497	0
Rab5c	NM_024456	3.8966	3.64781	0.24879	1.773	0
Car3	NM_007606	1.7327	1.0611	0.6716	4.694	0
Tcf25	NM_025804	4.661	4.46511	0.19589	1.569	0.0046
Lmnb1	NM_010721	3.7832	3.55731	0.22589	1.682	0.0663
Rpo1-2	NM_009086	2.7401	2.4276	0.3125	2.053	0
Odf2	BC057001	3.2338	2.9739	0.2599	1.819	0.0006
Sympk	BC049852	3.4027	3.15771	0.24499	1.757	0
Odf2	BC057001	2.9472	2.6675	0.2797	1.904	0.003
Tcf25	NM_025804	3.9199	3.71601	0.20389	1.599	0.0164
Mpst	NM_138670	3.2991	3.0624	0.2367	1.724	0
Setd5	NM_028385	4.1714	3.9884	0.183	1.524	0
Gm1752	XM_001003685	2.0884	1.6978	0.3906	2.458	0
Tspyl1	NM_009433	3.9586	3.7672	0.1914	1.553	0.0002
Nans	NM_053179	3.4225	3.20001	0.22249	1.669	0
Med18	NM_026039	2.9089	2.6437	0.2652	1.841	0.0001
2810482G21Rik	AK122545	2.7054	2.419	0.2864	1.933	0
Arl6ip5	NM_022992	3.7976	3.5997	0.1979	1.577	0.0004
Vamp3	NM_009498	2.5043	2.1942	0.3101	2.042	0.0005
Rab3d	NM_031874	2.7433	2.46791	0.27539	1.885	0

Symbol	Annotation	Mean (S80A)	Mean (WT)	Log Ratio	Fold Change	FDR
Rian	AK017440	3.5411	3.3383	0.2028	1.595	0.0145
AK143126	AK143126	2.2967	1.9704	0.3263	2.119	0
Tatdn2	NM_001033463	2.9354	2.6879	0.2475	1.768	0
AK046873	AK046873	2.3955	2.0872	0.3083	2.033	0
NAP057026-1	NAP057026-1	2.404	2.09791	0.30609	2.023	0
Rnf20	NM_182999	3.1599	2.94071	0.21919	1.656	0.0014
Zswim6	BC021311	2.9449	2.70991	0.23499	1.717	0
Fgr	NM_010208	2.0997	1.75521	0.34449	2.21	0.0007
Igsf4c	NM_153112	3.6004	3.4112	0.1892	1.545	0
5830457O10Rik	NM_145412	2.5089	2.2319	0.277	1.892	0
Supt7l	NM_028150	2.0734	1.73091	0.34249	2.2	0
B4galt7	NM_146045	2.6143	2.3541	0.2602	1.82	0
Polh	NM_030715	1.5822	1.1015	0.4807	3.024	0
Vapb	NM_019806	2.4449	2.1668	0.2781	1.897	0
Mapk8ip1	NM_011162	3.2656	3.0659	0.1997	1.583	0.0603
Cntn2	NM_177129	3.8167	3.6481	0.1686	1.474	0.0002
2610200G18Rik	NM_025998	2.3788	2.10021	0.27859	1.899	0
LOC665155	XM_976391	1.7638	1.3713	0.3925	2.468	0
Kif15	NM_010620	2.7726	2.5416	0.231	1.702	0.0004
Lix1	BC063057	2.5354	2.2814	0.254	1.794	0.0003
Cplx2	NM_009946	3.1035	2.9004	0.2031	1.596	0.0052
Snap29	NM_023348	3.6546	3.48381	0.17079	1.481	0.0011
AK050977	AK050977	2.6763	2.43881	0.23749	1.727	0
Fgd4	AK042588	2.0955	1.78331	0.31219	2.052	0.0001
Bloc1s3	NM_177692	2.5802	2.3345	0.2457	1.76	0
Med18	NM_026039	2.713	2.48221	0.23079	1.701	0.0001
Ly6h	NM_011837	3.5055	3.3301	0.1754	1.497	0.0184
Aco1	NM_007386	2.4103	2.14741	0.26289	1.831	0.0001
Lsm14b	NM_177727	2.6059	2.36521	0.24069	1.74	0.0035
Pafah1b1	NM_013625	4.2438	4.1015	0.1423	1.387	0.0031
Ufd1l	NM_011672	2.583	2.3464	0.2366	1.724	0.0305
Stk32c	NM_021302	1.8192	1.46541	0.35379	2.258	0
Pigt	NM_133779	4.1392	3.99691	0.14229	1.387	0.0209
Raf1	AK036317	2.5964	2.36601	0.23039	1.699	0
TC1522927	TC1522927	1.9304	1.60751	0.32289	2.103	0
Psmd9	NM_026000	2.8406	2.63381	0.20679	1.609	0.0256
TC1477251	TC1477251	1.434	0.97431	0.45969	2.881	0.0003
E430012M05Rik	AK051077	1.5833	1.19081	0.39249	2.468	0.0124
G430041M01Rik	NM_198102	2.9468	2.7561	0.1907	1.551	0
Rad1	NM_011232	2.7436	2.5401	0.2035	1.597	0.0003
AK043110	AK043110	2.6822	2.4751	0.2071	1.611	0.0221
AK084126	AK084126	1.3788	0.9132	0.4656	2.921	0.0018
ENSMUST00000088292	ENSMUST00000088292	2.8102	2.6148	0.1954	1.568	0.0101
Rgs16	NM_011267	2.9383	2.75491	0.18339	1.525	0
Jub	NM_010590	2.1749	1.92241	0.25249	1.788	0.0836
Cdk6	NM_009873	1.64	1.28761	0.35239	2.251	0.0089
ENSMUST00000066134	ENSMUST00000066134	3.6712	3.52821	0.14299	1.389	0.003
Peo1	NM_153796	1.6882	1.35021	0.33799	2.177	0
Rab11b	NM_008997	2.5199	2.30881	0.21109	1.625	0.0387
U2af2	NM_133671	2.1962	1.9526	0.2436	1.752	0.0017
Vamp3	NM_009498	2.1184	1.86551	0.25289	1.79	0.0812
Hnrpa0	AK019388	3.069	2.90181	0.16719	1.469	0.001
Zbtb12	NM_198886	4.1052	3.9825	0.1227	1.326	0.0645
Paxip1	NM_018878	1.4839	1.09991	0.38399	2.42	0.0199
Sh3bp2	NM_011893	2.5914	2.39321	0.19819	1.578	0.0236
Map3k10	XM_887283	3.5426	3.4005	0.1421	1.387	0.0073
Gas2l3	AK018456	2.6355	2.44181	0.19369	1.562	0.0374
2410081M15Rik	NM_028603	3.025	2.85821	0.16679	1.468	0.0006
Gabbr1	BC054735	2.8551	2.6808	0.1743	1.493	0.0272
Slc8a2	NM_148946	2.2588	2.03411	0.22469	1.677	0.0006
Ing3	NM_023626	2.5752	2.3815	0.1937	1.562	0.0009
6430526N21Rik	NM_001033383	2.4639	2.2607	0.2032	1.596	0.0015
Srebf2	NM_033218	3.0197	2.85781	0.16189	1.451	0.0002
Ube2b	AK135056	2.3598	2.15171	0.20809	1.614	0

Symbol	Annotation	Mean (S80A)	Mean (WT)	Log Ratio	Fold Change	FDR
Ccdc49	NM_026186	2.6446	2.4617	0.1829	1.523	0.0058
Bcl9	AK147659	2.4209	2.2216	0.1993	1.582	0.0004
AK169992	AK169992	1.9518	1.69871	0.25309	1.79	0.0005
Rbm9	NM_175387	3.4147	3.27721	0.13749	1.372	0.0005
Metrn	NM_133719	3.0922	2.9404	0.1518	1.418	0.0077
Chst7	NM_021715	2.5493	2.3629	0.1864	1.536	0.0053
Polr3gl	NM_027241	3.597	3.46741	0.12959	1.347	0.0483
BB113933	BB113933	3.0154	2.8596	0.1558	1.431	0.0004
Hnrpa0	AK019388	2.4619	2.26901	0.19289	1.559	0.0085
Olig1	NM_016968	3.0919	2.9429	0.149	1.409	0.0103
3110032G18Rik	NM_028443	1.8358	1.5726	0.2632	1.833	0.0595
Ttll1	NM_178869	3.1082	2.9612	0.147	1.402	0.0623
Dync1li1	NM_146229	2.9134	2.7571	0.1563	1.433	0.0985
Cyp26a1	NM_007811	1.3164	0.9226	0.3938	2.476	0.0314
Osbpl8	NM_175489	2.6326	2.46051	0.17209	1.486	0.0237
AK030273	AK030273	2.6977	2.5313	0.1664	1.466	0.0011
BC024868	NM_199149	3.0649	2.9198	0.1451	1.396	0.04
C1qtnf2	NM_026979	1.3213	0.93851	0.38279	2.414	0.1
Cxadr	NM_001025192	3.2273	3.0925	0.1348	1.363	0.0016
Fbln2	NM_007992	2.7746	2.61891	0.15569	1.431	0.0062
Acads	NM_007383	2.1065	1.897	0.2095	1.619	0.0029
ENSMUST00000098637	ENSMUST00000098637	2.3	2.11051	0.18949	1.546	0.005
4930533I22Rik	AK029757	1.4741	1.15661	0.31749	2.077	0.0865
Fbxo30	NM_027968	3.0447	2.905	0.1397	1.379	0.008
Hirip5	AK081950	1.4582	1.1396	0.3186	2.082	0.0575
Slc27a1	NM_011977	2.946	2.8021	0.1439	1.392	0.0015
Tigd3	NM_198634	1.7684	1.51781	0.25059	1.78	0.01
0610011I04Rik	NM_025326	2.0326	1.8194	0.2132	1.633	0.006
Ecm2	NM_001012324	1.4639	1.15061	0.31329	2.057	0.0744
Jmjd2a	NM_172382	2.4943	2.328	0.1663	1.466	0.056
Igf2bp1	NM_009951	2.6447	2.48871	0.15599	1.432	0.001
Zfp146	NM_011980	2.1809	1.98901	0.19189	1.555	0.0016
C79127	NM_177691	1.7607	1.51971	0.24099	1.741	0.0157
2810474O19Rik	NM_026054	3.6486	3.53901	0.10959	1.287	0.0083
AK129128	AK079259	1.3877	1.0695	0.3182	2.08	0.0452
Neb1	AK077332	1.4086	1.0965	0.3121	2.051	0.0516
C130021H21Rik	AK047913	1.2775	0.9242	0.3533	2.255	0.077
Unc5b	NM_029770	2.1387	1.9494	0.1893	1.546	0.0006
Gtpbp3	NM_032544	2.865	2.7274	0.1376	1.372	0.056
1600027J07Rik	AK005548	1.2239	0.85361	0.37029	2.345	0.0509
Atp1a1	NM_144900	4.056	3.96011	0.09589	1.247	0.0679
Cdc42l	NM_146040	1.6623	1.4124	0.2499	1.777	0.0192
A_52_P893105	A_52_P893105	1.9018	1.68781	0.21399	1.636	0.0011
TC1521263	TC1521263	2.532	2.37571	0.15629	1.433	0.001
1500009C09Rik	XM_901682	2.6204	2.4701	0.1503	1.413	0.0086
Trip10	NM_134125	1.3637	1.04631	0.31739	2.076	0.022
Zic1	NM_009573	3.0761	2.94931	0.12679	1.339	0.0374
BU562039	BU562039	2.7349	2.59161	0.14329	1.39	0.0243
Cyp20a1	NM_030013	2.3133	2.1424	0.1709	1.482	0.0086
Gipr	AK146552	1.3041	0.9693	0.3348	2.161	0.0413
Igf1r	NM_010513	2.5654	2.41351	0.15189	1.418	0.0198
A430107D22Rik	AK041479	1.483	1.2061	0.2769	1.891	0.0955
Wasl	NM_028459	2.504	2.35151	0.15249	1.42	0.0006
Carkl	NM_029031	1.3983	1.1028	0.2955	1.974	0.0648
Soat1	NM_009230	1.9139	1.71101	0.20289	1.595	0.0405
Myo18b	AK016515	1.4947	1.2247	0.27	1.862	0.0664
AI461788	AK028016	1.2278	0.8805	0.3473	2.224	0.0418
Taok1	BC047271	4.0213	3.93001	0.09129	1.233	0.0615
Mical2	NM_177282	1.743	1.5209	0.2221	1.667	0.0483
D1Bwg0212e	NM_028043	1.9498	1.7541	0.1957	1.569	0.0858
Cecam1	NM_207298	1.9488	1.7543	0.1945	1.564	0.018
Tbc1d9	NM_027758	1.777	1.56151	0.21549	1.642	0.0147
Ube4a	AK172893	3.231	3.1184	0.1126	1.295	0.0972
Tnfaip6	NM_009398	2.1466	1.97661	0.16999	1.479	0.0718

Symbol	Annotation	Mean (S80A)	Mean (WT)	Log Ratio	Fold Change	FDR
Lrrq2	AK078361	1.7914	1.5851	0.2063	1.608	0.0958
Kpna4	NM_008467	1.82	1.6176	0.2024	1.593	0.0272
Snf1lk	NM_010831	2.6865	2.5556	0.1309	1.351	0.0362
0710001B24Rik	NM_175118	2.6386	2.50531	0.13329	1.359	0.0322
BC021831	BC021831	1.8534	1.65831	0.19509	1.567	0.0304
Cnr1	NM_007726	2.3633	2.2138	0.1495	1.41	0.0039
AK044799	AK044799	1.892	1.70171	0.19029	1.549	0.0077
TC1440691	TC1440691	2.4368	2.29251	0.14429	1.394	0.0051
Calcoco1	NM_026192	1.9762	1.79781	0.17839	1.507	0.024
Rdh13	AK089458	2.0336	1.86151	0.17209	1.486	0.0063
Zbtb24	AF263010	2.3131	2.1651	0.148	1.406	0.0088
Arvcf	NM_033474	2.904	2.78831	0.11569	1.305	0.0036
AK037868	AK037868	1.7816	1.5865	0.1951	1.567	0.0431
Mapk8	NM_016700	2.2339	2.0824	0.1515	1.417	0.0488
Traf3ip2	NM_134000	1.2189	0.9126	0.3063	2.024	0.0523
AK016486	AK016486	2.2479	2.09901	0.14889	1.408	0.0985
Peg3	NM_008817	2.1974	2.046	0.1514	1.417	0.0292
Tmem142c	NM_198424	2.5943	2.4677	0.1266	1.338	0.06
2810449C10Rik	AK039679	3.178	3.07561	0.10239	1.265	0.06
Psmc2	AK083989	2.0893	1.9308	0.1585	1.44	0.0806
Mare	NM_181569	2.4599	2.3285	0.1314	1.353	0.0943
Snx27	AK147452	1.8533	1.67501	0.17829	1.507	0.0359
D030051J21Rik	AK083595	1.1949	0.8988	0.2961	1.977	0.0346
Amdhd2	AK078259	2.3977	2.2649	0.1328	1.357	0.0896
Mirg	AK077315	2.2298	2.08701	0.14279	1.389	0.0837
AK031010	AK031010	2.1712	2.02431	0.14689	1.402	0.0819
Mnab	XM_130233	2.9115	2.8037	0.1078	1.281	0.0679
Chd1	NM_007690	2.1572	2.01	0.1472	1.403	0.0477
Gsk3b	NM_019827	2.3586	2.22501	0.13359	1.36	0.0127
Snap25	NM_011428	2.867	2.7598	0.1072	1.279	0.0807
Lrrc57	NM_025657	2.3637	2.2332	0.1305	1.35	0.0094
TC1526069	TC1526069	2.6199	2.5033	0.1166	1.307	0.0813
Brunol5	AK132321	1.7376	1.5584	0.1792	1.51	0.0686
AK081327	AK081327	1.1614	0.87481	0.28659	1.934	0.0667
Pcd6ip	NM_011052	1.8144	1.6479	0.1665	1.467	0.0937
Stch	NM_030201	2.8925	2.7943	0.0982	1.253	0.024
6530418L21Rik	NM_175398	2.3024	2.17911	0.12329	1.328	0.0649
6430704M03Rik	AK078331	2.1056	1.97551	0.13009	1.349	0.0483
Zfhx1b	AK031541	2.104	1.9768	0.1272	1.34	0.0794
L1cam	NM_008478	2.1029	1.98311	0.11979	1.317	0.0806
Cdyl2	NM_029441	2.0069	1.8819	0.125	1.333	0.0918

The genes that are of low abundance (mean value < 1.7) are in bold. The mean value of wild-type and S80A is the logarithm of the raw reading to the base of 10. The raw reading can be calculated as $10^{\text{mean value}}$. The log ratio is the logarithm of the ratio of S80A versus wild-type to the base of 10. The fold change can be calculated as $10^{\log \text{ratio}}$.

Table S3. The lists of genes that are down-regulated in S80A samples compared with wild-type samples which may contain multiple probes targeting the same gene

Symbol	Annotation	Mean (S80A)	Mean (WT)	Log ratio	Fold change	FDR
Genes that are down-regulated in S80A samples compared with wild-type samples (FDR < 0.05)						
Gpr17	NM_001025381	2.1903	2.81159	-0.62129	4.181	0.0022
Anp32a	NM_009672	2.4009	2.96939	-0.56849	3.702	0
Defb37	NM_181683	2.2313	2.6084	-0.3771	2.382	0
Lgi4	NM_144556	1.6943	2.1524	-0.4581	2.871	0
Gstm1	NM_010358	3.6954	3.911	-0.2156	1.642	0
Cmtm5	NM_026066	2.1925	2.53209	-0.33959	2.185	0
Gstm3	NM_010359	3.1915	3.4114	-0.2199	1.659	0.002
Abhd3	NM_134130	1.6106	2.00629	-0.39569	2.487	0
Bcas1	NM_029815	1.8036	2.14449	-0.34089	2.192	0.0003
Cot11	NM_028071	4.5576	4.6993	-0.1417	1.385	0.0017
Gstm1	NM_010358	2.1509	2.43199	-0.28109	1.91	0.0006
Pla2g7	NM_013737	2.3674	2.62489	-0.25749	1.809	0
Olfr1386	NM_001011741	1.3004	1.711	-0.4106	2.573	0.0029
Havcr2	NM_134250	1.6664	1.99589	-0.32949	2.135	0.034
Rarres1	XM_130987	1.1222	1.54869	-0.42649	2.669	0.0073
TC1414310	TC1414310	3.0491	3.22729	-0.17819	1.507	0.0135
Bdh2	NM_027208	1.3999	1.7527	-0.3528	2.253	0.0002
Bdh2	NM_027208	2.1042	2.34929	-0.24509	1.758	0
Padi2	NM_008812	1.4318	1.7685	-0.3367	2.171	0.0053
ENSMUST00000089796	ENSMUST00000089796	1.6158	1.9189	-0.3031	2.009	0.0073
Cbx7	NM_144811	2.1293	2.35519	-0.22589	1.682	0.0227
Oas3	NM_145226	1.0631	1.4557	-0.3926	2.469	0.0019
Cldn10	NM_021386	1.6794	1.9516	-0.2722	1.871	0.0244
Aph1a	NM_146104	2.3135	2.51609	-0.20259	1.594	0.0418
Slc36a3	NM_172258	0.9503	1.3624	-0.4121	2.582	0.0006
Fxyd1	NM_019503	1.0799	1.45259	-0.37269	2.358	0.015
AU042671	XM_132325	2.3868	2.57049	-0.18369	1.526	0.0034
AK047230	AK047230	1.6382	1.89399	-0.25579	1.802	0.0048
1700018B24Rik	NM_025493	1.9369	2.15569	-0.21879	1.654	0.0002
AV254721	AV254721	2.4569	2.62939	-0.17249	1.487	0.0115
Nlk	NM_008702	3.1975	3.331	-0.1335	1.359	0.007
Arts1	NM_030711	1.4373	1.71249	-0.27519	1.884	0.0119
Zcchc11	NM_175472	1.5366	1.7927	-0.2561	1.803	0.0045
TC1463322	TC1463322	2.7406	2.89009	-0.14949	1.41	0.0472
Ncoa6	NM_019825	2.1324	2.31899	-0.18659	1.536	0.0002
Mbp	NM_010777	1.4774	1.7349	-0.2575	1.809	0.0169
6330500D04Rik	AK134538	2.4638	2.62469	-0.16089	1.448	0.0106
Prdm16	NM_027504	1.8106	2.02079	-0.21019	1.622	0.0071
Slc30a1	NM_009579	2.7928	2.93309	-0.14029	1.381	0.0151
4930467M19Rik	AK015524	2.2105	2.3852	-0.1747	1.495	0.0241
A_51_P462771	A_51_P462771	1.9967	2.1867	-0.19	1.548	0.0407
AK034829	AK034829	0.9013	1.2654	-0.3641	2.312	0.0458
Nav1	NM_173437	1.9589	2.14809	-0.18919	1.545	0.0037
Ntsr2	NM_008747	1.4703	1.7141	-0.2438	1.753	0.0207
cf7l2	NM_009333	2.602	2.7445	-0.1425	1.388	0.0231
D230040A04Rik	AK039302	2.1293	2.30119	-0.17189	1.485	0.0145
Itgb8	NM_901358	1.7782	1.979	-0.2008	1.587	0.0345
AK040092	AK040092	0.8551	1.21639	-0.36129	2.297	0.0469
Srgap3	NM_080448	1.5344	1.76099	-0.22659	1.684	0.0492
Eaf2	NM_134111	2.1012	2.26189	-0.16069	1.447	0.0271
1500015O10Rik	NM_024283	3.1684	3.27669	-0.10829	1.283	0.0249
MGC54654	NM_001004170	0.8774	1.20019	-0.32279	2.102	0.0211
Pacrg	NM_027032	2.1533	2.30289	-0.14959	1.411	0.0042
S100b	NM_009115	1.9033	2.0695	-0.1662	1.466	0.0444
Dhrs8	NM_053262	2.3883	2.52249	-0.13419	1.362	0.0062
1700054F22Rik	XM_485380	1.0183	1.29889	-0.28059	1.908	0.0322
1700007K13Rik	BC099566	2.3705	2.493	-0.1225	1.325	0.0122
4933412F11Rik	AK016790	1.8727	2.02099	-0.14829	1.406	0.0109
Eif2ak1	AK032508	2.7966	2.8953	-0.0987	1.255	0.027

Symbol	Annotation	Mean (S80A)	Mean (WT)	Log ratio	Fold change	FDR
Genes that are down-regulated in S80A samples compared with wild-type samples (FDR < 0.1)						
Gpr17	NM_001025381	2.1903	2.81159	-0.62129	4.181	0.0022
Anp32a	NM_009672	2.4009	2.96939	-0.56849	3.702	0
Defb37	NM_181683	2.2313	2.6084	-0.3771	2.382	0
Lgi4	NM_144556	1.6943	2.1524	-0.4581	2.871	0
Gstm1	NM_010358	3.6954	3.911	-0.2156	1.642	0
Cmtm5	NM_026066	2.1925	2.53209	-0.33959	2.185	0
Apoe	NM_009696	3.9569	4.1444	-0.1875	1.539	0.0942
Gstm3	NM_010359	3.1915	3.4114	-0.2199	1.659	0.002
Abhd3	NM_134130	1.6106	2.00629	-0.39569	2.487	0
Bcas1	NM_029815	1.8036	2.14449	-0.34089	2.192	0.0003
Cot11	NM_028071	4.5576	4.6993	-0.1417	1.385	0.0017
Gstm1	NM_010358	2.1509	2.43199	-0.28109	1.91	0.0006
Pla2g7	NM_013737	2.3674	2.62489	-0.25749	1.809	0
Olfr1386	NM_001011741	1.3004	1.711	-0.4106	2.573	0.0029
Havcr2	NM_134250	1.6664	1.99589	-0.32949	2.135	0.034
Rarres1	XM_130987	1.1222	1.54869	-0.42649	2.669	0.0073
Masp2	NM_001003893	1.1636	1.5778	-0.4142	2.595	0.056
Mt2	NM_008630	4.187	4.32029	-0.13329	1.359	0.0715
TC1414310	TC1414310	3.0491	3.22729	-0.17819	1.507	0.0135
Bdh2	NM_027208	1.3999	1.7527	-0.3528	2.253	0.0002
Bdh2	NM_027208	2.1042	2.34929	-0.24509	1.758	0
Padi2	NM_008812	1.4318	1.7685	-0.3367	2.171	0.0053
ENSMUST00000089796	ENSMUST00000089796	1.6158	1.9189	-0.3031	2.009	0.0073
Cbx7	NM_144811	2.1293	2.35519	-0.22589	1.682	0.0227
Oas3	NM_145226	1.0631	1.4557	-0.3926	2.469	0.0019
Cldn10	NM_021386	1.6794	1.9516	-0.2722	1.871	0.0244
Aph1a	NM_146104	2.3135	2.51609	-0.20259	1.594	0.0418
Spn	NM_009259	0.9043	1.33759	-0.43329	2.712	0.0865
Slc36a3	NM_172258	0.9503	1.3624	-0.4121	2.582	0.0006
Fxyd1	NM_019503	1.0799	1.45259	-0.37269	2.358	0.015
Snrpd3	NM_026095	4.0178	4.13009	-0.11229	1.295	0.0911
AU042671	XM_132325	2.3868	2.57049	-0.18369	1.526	0.0034
AK047230	AK047230	1.6382	1.89399	-0.25579	1.802	0.0048
1700018B24Rik	NM_025493	1.9369	2.15569	-0.21879	1.654	0.0002
AK090167	AK090167	0.9263	1.3238	-0.3975	2.497	0.0543
AV254721	AV254721	2.4569	2.62939	-0.17249	1.487	0.0115
Nlk	NM_008702	3.1975	3.331	-0.1335	1.359	0.007
Arts1	NM_030711	1.4373	1.71249	-0.27519	1.884	0.0119
Aig1	NM_025446	1.6901	1.926	-0.2359	1.721	0.0539
Zcchc11	NM_175472	1.5366	1.7927	-0.2561	1.803	0.0045
TC1463322	TC1463322	2.7406	2.89009	-0.14949	1.41	0.0472
6430510M02Rik	NM_176932	2.4185	2.5846	-0.1661	1.465	0.094
Ncoa6	NM_019825	2.1324	2.31899	-0.18659	1.536	0.0002
Mbp	NM_010777	1.4774	1.7349	-0.2575	1.809	0.0169
6330500D04Rik	AK134538	2.4638	2.62469	-0.16089	1.448	0.0106
Prdm16	NM_027504	1.8106	2.02079	-0.21019	1.622	0.0071
Slc30a1	NM_009579	2.7928	2.93309	-0.14029	1.381	0.0151
4930467M19Rik	AK015524	2.2105	2.3852	-0.1747	1.495	0.0241
A_51_P462771	A_51_P462771	1.9967	2.1867	-0.19	1.548	0.0407
AK034829	AK034829	0.9013	1.2654	-0.3641	2.312	0.0458
Nav1	NM_173437	1.9589	2.14809	-0.18919	1.545	0.0037
Ntsr2	NM_008747	1.4703	1.7141	-0.2438	1.753	0.0207
Olfr1198	NM_207567	2.1738	2.34379	-0.16999	1.479	0.0759
Tcf7l2	NM_009333	2.602	2.7445	-0.1425	1.388	0.0231
D23040A04Rik	AK039302	2.1293	2.30119	-0.17189	1.485	0.0145
TC1521782	TC1521782	1.6203	1.84	-0.2197	1.658	0.0837
Itgb8	XM_901358	1.7782	1.979	-0.2008	1.587	0.0345
AK040092	AK040092	0.8551	1.21639	-0.36129	2.297	0.0469
Srgap3	NM_080448	1.5344	1.76099	-0.22659	1.684	0.0492
Bhlhb5	NM_021560	3.9633	4.0561	-0.0928	1.238	0.0884
Unkl	AK054549	1.7797	1.97349	-0.19379	1.562	0.074
BC018371	NM_153807	2.8444	2.9691	-0.1247	1.332	0.0937
AK082760	AK082760	1.5209	1.739	-0.2181	1.652	0.0808

Symbol	Annotation	Mean (S80A)	Mean (WT)	Log ratio	Fold change	FDR
Eaf2	NM_134111	2.1012	2.26189	-0.16069	1.447	0.0271
Mgll	NM_011844	2.8803	2.99939	-0.11909	1.315	0.0624
1500015O10Rik	NM_024283	3.1684	3.27669	-0.10829	1.283	0.0249
BC089491	NM_175033	1.4002	1.6305	-0.2303	1.699	0.0531
C630050I24Rik	AK021281	2.2972	2.4403	-0.1431	1.39	0.0797
Lims2	NM_144862	2.1005	2.2548	-0.1543	1.426	0.0719
MGC54654	NM_001004170	0.8774	1.20019	-0.32279	2.102	0.0211
Pacrg	NM_027032	2.1533	2.30289	-0.14959	1.411	0.0042
S100b	NM_009115	1.9033	2.0695	-0.1662	1.466	0.0444
Dhrs8	NM_053262	2.3883	2.52249	-0.13419	1.362	0.0062
1700054F22Rik	XM_485380	1.0183	1.29889	-0.28059	1.908	0.0322
Pglyrp1	NM_009402	0.8433	1.1568	-0.3135	2.058	0.0546
Cryaa	NM_013501	0.9208	1.2132	-0.2924	1.96	0.0957
1700007K13Rik	BC099566	2.3705	2.493	-0.1225	1.325	0.0122
4933412F11Rik	AK016790	1.8727	2.02099	-0.14829	1.406	0.0109
Kifc1	NM_053173	2.8607	2.95869	-0.09799	1.253	0.0619
4931406H21Rik	NM_175264	1.0323	1.2782	-0.2459	1.761	0.0783
Eif2ak1	AK032508	2.7966	2.8953	-0.0987	1.255	0.027
Ttc22	NM_177667	0.8526	1.1045	-0.2519	1.786	0.0542

The genes that are of low abundance (mean value < 1.7) are in bold. The mean value of wild-type and S80A is the logarithm of the raw reading to the base of 10. The raw reading can be calculated as $10^{\text{mean value}}$. The log ratio is the logarithm of the ratio of S80A versus wild-type to the base of 10. The fold change can be calculated as $10^{\log \text{ratio}}$.